PREPRINT of the paper, published in:

Journal of Colloid and Interface Science. 2005. Vol.285. Iss.2. P.795-803

Excess density in oilfield water - crude oil dispersions

Igor N. Evdokimov,[a,]* Nikolaj Yu. Eliseev[a] and Valerij A. Iktisanov[b]

[a]*Department of Physics, Gubkin Russian State University of Oil and Gas, Leninsky Prospekt, 65, Moscow B-296, GSP-1, 119991, Russia;*

[b]*TATNIPINEFT Institute, ul. Musa Dzhalil, 32, Bugulma, Tatarstan 423236, Russia*

---

* Corresponding author. *E-mail address*: physexp@gubkin.ru

Abstract

Extensive density measurements were performed with mixtures of 12 degassed (dead) crude oils with respective oilfield brines (formation waters). All unprocessed samples were collected directly from well-heads and contained only indigenous surfactants, such as asphaltenes and fine solids. Non-zero excess densities and excess thermal expansions (evaluated in the assumption of quasi-binary water-oil mixtures) were observed for water cuts in the range from X=0.4 to X=0.6 at all studied temperatures of T=5-50^{o}C. We suggest that these results are due to a formation of some dense asphaltene-mediated "middle phase" in the studied w/o dispersions. This suggestion is substantiated by plotting T-X phase diagrams which topologically strongly resemble those conventionally observed in some standard Winsor III-type systems. The formation of a complexly-structured "middle phase" has been directly verified by preliminary visual/microscopic studies of a phase separation in a crude oil – water mixture

Keywords: Crude oil; Brine; Dispersion; Emulsion; Viscosity; Excess density; Middle phase; Bicontinuous phase; Asphaltenes;

1. Introduction

The output of a production oil well consists typically of a dispersion of formation water (brine) in a crude oil. The knowledge of the physical properties of water/crude oil dispersions is necessary if the behaviour and characteristics of their multiphase flows are to be predicted correctly. These properties are essential for the interpretation of rheological experiments, for development of multiphase metering devices and for equipment and pipeline design [1-3]. Depending on the water cut and the flow conditions, water/oil dispersions may exhibit transitions among a variety of phase states; in the presence of surfactants, stable emulsions may be formed [4-8]. A well-known type of a phase transition in a water/oil mixture is that of a phase inversion from a w/o to a o/w dispersion [1,9-11]. The phase transitions are usually accompanied by noticeable anomalies of some mixture's properties and may be the cause of a significant increase in the pressure gradient in a flowing fluid, of undesirable stability of w/o or o/w emulsions etc. In spite of an extensive research, the microscopic phenomena near the phase transitions are still poorly understood (cf. a recent review [11]). In particular, there is a large diversity of data for oil/brine dispersions from different well-streams, apparently due to different contents of the "indigenous surfactants" in crude oils, such as asphaltenes, resins and fine solids [12]. It is suggested, that some of these indigenous components may be responsible for specific structural transitions in oilfield w/o mixtures, which precede a phase inversion and resemble the phenomena of formation of "middle phase" microemulsions (Winsor III systems) in model mixtures [11]. Apparently, for oilfield practitioners, dealing with heavy oils and bituminous oilsands, formation of three-phase systems in non-flowing oil-brine mixtures is a well-known phenomenon, the middle (macro)emulsion phase most frequently referred to as the "rag layer".

Although “rag layers” are the cause of costly problems in performance of dewatering/desalting equipment, only recently these pre-inversion middle phases became objects of systematic experimental investigations [13,14].

Presently, the main method of studying phase transformations in crude oil/water mixtures is that of rheological measurements [1-11,15,16]. It has been repeatedly demonstrated that rheological technique offer means to determine the inner structure of emulsions and provide evidence of the technologically important structural changes. The main drawback of this technique is the presence of a fluid flow which may noticeably change the structural properties of an oil/water mixture [1,2,15]. Due to continuous mechanical agitation, flowing dispersions may be dynamically stabilised [17] and may exhibit the properties close to those of stable emulsions.

Phase diagrams of non-flowing oil/water mixtures most frequently are investigated by straightforward visualisation techniques [18-21]. These techniques are favoured owing to the ease of interpretation; however the volumes of visibly distinct phases can not be determined with high precision. Moreover, in dark heavy oil or bitumen mixtures some of these phases are visually indistinguishable.

To reveal the details of the phase behaviour, it may be useful to apply to a crude oil/brine system, in spite of it compositional complexity, some of the approaches developed for binary liquid-liquid mixtures. Specific molecular interactions in binary mixtures are successfully interpreted on the basis of the Prigogine–Flory–Patterson (PFP) model [22-24], where thermodynamic/interaction parameters are related to measurable macroscopic properties through the so-called excess functions, e.g. the excess molar volume V_m^E . In practice, the values of V_m^E for mixtures of components with well-known molecular weights are calculated from the

corresponding density measurements. For such complex components as crude oil and formation water (brine) molecular weights can not be strictly defined, hence it seems more appropriate to analyse the mixtures not in terms of excess molar volumes but directly in terms of excess densities.

In view of the above arguments, a technique of detailed density measurements (and evaluation of the corresponding excess functions), well developed for simple binary solutions/mixtures, may be applied for studying more complex crude oil/brine mixtures. Though this suggestion may seem trivial, a review of the available (English and Russian – language) literature did not reveal any relevant publications. Hence, the present work was aimed at producing new results of density-structure relationships in industrial crude oil-brine mixtures.

2. Experimental

2.1. Samples

The studied crude oil and brine samples were collected from the well-heads at the newly-developed Aktanishskoje oil reservoir, Tatarstan, Russia and have been supplied by the TATNEFT oil company. The basic physicochemical properties of these 12 samples (determined by the supplier) are listed in the upper lines of Table 1. The samples are denoted according to the corresponding productive layers: T – "Tulskij"; B – "Bobrikovskij"; K – "Kizelovskij". The next two digits denote the individual number of the well, the last two ones – the year of the sampling. It can be seen, that according to standard classification schemes (e.g. that of Tissot and Welte [25]), all crudes may be classified as "heavy sour" with densities in the range of ≈897-908 kg/m^3 and sulphur contents above 3 wt. %. All brines are strongly mineralised and exhibit densities of 1148-1175 kg/m^3 , i.e. salt contents of about 150 g/litre, which

is somewhat higher, but close to the values typical for other studies of crude oil/brine mixtures [1]. The bottom line in Table 1 shows the properties of the "Romashkinskoje" sample, employed in phase separation experiments (cf. Section 3.8).

2.2 Apparatus and procedure

The experimental investigation of oil/brine mixtures has been performed at the TATNIPINEFT Scientific Research Institute with the primary goal to update a database for reservoir modelling of the new Aktanishskoje oilfield. Hence the ranges of investigated water cuts and temperatures were those, encountered in the oil production processes, namely maximum water cuts of 0.6 and fluid temperatures of 5-50^{o}C. All oils and brines were stored at room temperature. In each experiment, some quantities of both liquids were preheated/precooled to the measurement's temperature and samples with the required water cuts were mixed (at this temperature) for several minutes in a conventional magnetic stirrer. Both viscosity and density measurements commenced within 1 minute after homogenising the samples and no visible phase separation was registered in course of any experiment.

The dynamic viscosities of all samples have been measured with a temperature-controlled METTLER Reomat RM-180 viscometer for shear rates of 6-80 s^{-1} . At each mixture's temperature, the measurements proceeded in an ascending-rate order.

Densities of pure components and of oil/brine mixtures were determined in a temperature-controlled closet by using a standard 10 ml pycnometer, weighed with an accuracy of 0.1 mg. The relative excess density ρ^{E}_{R} for any water cut X was

calculated from the measured values of the densities of the liquid mixture ρ_M , of the crude oil ρ_O and of the brine ρ_B , using an equation:

$$\rho^E_R = (\rho_M - \rho_{ID})/\rho_{ID} \quad (1)$$

where ρ_{ID} is a density of an ideal binary mixture of non-interacting components:

$$\rho_{ID} = \rho_O (1-X) + \rho_B X \quad (2)$$

3. Results and Discussion

3.1. Viscosity measurements

A detailed report on the viscosity experiments with oilfield water – crude oil mixtures will be published elsewhere. The results in this section are presented to provide a basis of comparison of our samples with w/o dispersions, rheologically investigated in earlier studies. Fig. 1 shows a representative dependence of viscosity η on a water cut X for the sample T6097, at 50^{o}C. All data were obtained for a shear rate of 80 s^{-1}, at the Newtonian viscosity plateaux above the shear-thinning ranges. The observed $\eta(X)$ dependence (filled circles) is much steeper than viscosity trends for w/o emulsions with non-interacting drops [26] predicted by the hydrodynamic Stokes-Einstein expression $\eta = \eta_{OIL} (1+ 2.5X)$ and by its quadratic expansion $\eta=\eta_{OIL} (1 + 2.5X +6X^2)$ (solid lines 1 and 2, respectively). The best fit to our data set (solid curve 3) was obtained by applying the Mooney expression for dispersions of interacting particles (water drops) [27,28] :

$$\eta_M = \eta_{OIL} \exp[2.5X/(1-mX)] \quad (3)$$

with the value of interaction parameter m equal to 0.83.

It has been repeatedly shown [1,9-11] that an inversion from an oil-continuous to a water-continuous dispersion is necessarily accompanied by a substantial (sometimes by orders of magnitude) viscosity reduction. In all our samples viscosities

gradually increased with increasing water cuts (as in Fig. 1), indicating that in no case an inversion occurred and that inversion points were above X=0.6. It should be noted that in some other studies of crude oil / brine mixtures inversion points were observed at lower water cuts, namely at X=0.45-0.55 [1], at X≈0.4 [2] and even at X=0.05 [21]. These differences may be attributed to individual properties of the crudes, as follows from an extensive study by Djuve et al. [21] of o/w mixtures with 13 crudes of various geographical origins. The data of [21] show that the main factors affecting an inversion water cut are crude's viscosity and asphaltene content. Inversion at X=0.05 was observed for crudes with negligible content of asphaltenes and with viscosities below 4 mPa·s (at 25^{o}C). In crudes with 2.6-3.6 wt. % asphaltenes and with η=10-17 mPa·s, inversion points increased to X=0.6. Hence, even higher inversion points may be expected for our samples (cf. Table 1) with 3.03-9.35 wt. % asphaltenes and viscosities of 37-64 mPa·s (at 20^{o}C).

For all samples at temperatures in the range of 5-50^{o}C the measured viscosity-water cut dependencies at the first glance looked like perfectly monotonous functions and did not show any evidence of some specific pre-inversion phase transformations. However, after such transformations were revealed by density studies, discussed in the following sections, it became reasonable to seek the presence of respective anomalies in the seemingly smooth viscosity dependencies.

Firstly, distinct peaking was revealed in the temperature dependence of the best-fit Mooney interaction parameters m, as shown in Fig. 2. A maximum at ≈30^{o}C is in a good agreement with extrema of excess densities in Fig. 6. Secondly, an evidence of some pre-inversion structural transformation was obtained by analysing the shear-thinning behaviour of brine/oil mixtures with increasing water cuts. As a measure of shear thinning we used the ratio of viscosities at the minimum and the

maximum shear rates (6 s^{-1} and 80 s^{-1}). Fig. 3 shows that at low water cuts the value of $\eta(6)/\eta(80)$ remains virtually constant, while above X=0.4 it starts to increase, indicating the appearance of some weakly bound structures, which are destroyed at high shear rates. Again, the results of Fig. 3 are in qualitative agreement with the excess density data, discussed in the following sections.

3.2. Density – water cut relationships

A linear relationship (2) of the density and water cut for crude oil – brine dispersions/emulsions (additivity law) is frequently implied and, in some cases, it is recommended for industrially-oriented calculations of multiphase flows even in cases of substantial water cuts [29]. However, for a majority of our samples anomalous deviations from linear $\rho_M(X)$ dependencies at water cuts of 0.4-0.6 were evident even before calculation of excess functions. The largest (positive) deviations from an additivity law were observed with the sample T6097 – for a water cut of 0.4, at 5^oC, the measured mixture's density ρ_M was by ≈ 17 kg/m^3 larger than ρ_{ID} calculated according to an additivity law (2). At 5^oC, positive deviations from an additivity law were observed in approximately 50% of the studied samples, though in most cases the magnitude of these deviations was so small, that they were revealed only by calculation of excess functions. An example is the sample T6199 for which the original $\rho_M(X)$ dependencies at first glance looked almost perfectly linear as the largest deviation of ρ_M from ρ_{ID} was as small as 2.6 kg/m^3 (for water cut 0.5, at 50^oC). Finally a sizeable part of the studied samples (e.g. the sample B4899) exhibited (at least, at some temperatures) negative deviations of ρ_M from ρ_{ID} , with clearly observed "depression" at the original $\rho_M(X)$ dependencies.

These above specific water cuts are close to inversion points observed in other studies of natural crude oil / brine dispersions [1,2,9,21], hence the observed density anomalies were regarded as indicative of some pre-inversion phase transformations in the studied samples.

3.3. Correlations of maximum excess densities with oil/brine properties

Maximum deviations from an additivity law for the studied samples (i.e. peak values of relative excess densities ρ^E_R) were tested for correlations with all crude oil/brine properties, listed in Table 1. We could not find any conclusive correlations with oil or brine density, oil molecular weight, or the contents of sulphur, resins and waxes. On the other hand, there appear to be definite correlations of ρ^E_R with oil asphaltene contents and with oil kinematic viscosities, as shown in Fig. 4 (test temperature 5^{o}C, water cuts 0.4 and 0.5 for asphaltene and viscosity correlations, respectively). The sufficiently high values of the coefficients of determination (R^2 = 0.552 and R^2 = 0.361) indicate that asphaltene contents and viscosities of oils indeed may be the major factors determining a non-ideality of crude oil / formation water mixtures. A notable feature of Fig. 4 is an apparent existence of a "critical asphaltene content" (≈5 wt. %) and of a "critical viscosity" (≈50 mm^2/s) which delimit the data subsets with negative and positive values of ρ^E_R .

3.4. Water cut effects on the excess densities

The measured densities of all studied samples with water cuts of X≤0.3 did not show any variations from an additivity law and these mixtures behaved like ideal binary ones with ρ^E_R = 0. Density anomalies, i.e. non-zero values of ρ^E_R, were registered only for water cuts of 0.4, 0.5 and 0.6, with maximum peaking of ρ^E_R at

X≈0.45-0.55 (pre-inversion transformations), as shown in Fig. 5 for some representative cases. The lines, connecting the data points, are drawn merely to guide the eye and have no special significance.

The highest absolute values of the excess density (ρ^E_R≈2%) in our studies were observed for the sample T6097 (Fig. 5a), where density anomalies remained high and positive at all fluid temperatures from 5^{o}C (open circles) to 50^{o}C (filled circles). In other samples with smaller density anomalies ρ^E_R may have remained positive (sample T6199, Fig. 5b) or negative in the entire temperature range studied, or may have changed sign at some specific temperature, as in case of sample B4899 (Fig. 5c).

3.5. Non-monotonous temperature effects on the excess densities

In all studied oil/brine samples, for any water cut with non-zero ρ^E_R values, we observed a common qualitative feature of temperature effect on the excess densities. Namely, all measured ρ^E_R exhibited distinct extrema (either minima or maxima) in the same comparatively narrow temperature range from ≈26^{o}C to ≈34^{o}C, as illustrated in Fig. 6a,b,c for a water cut of 0.4. In the previous sections, peaking of ρ^E_R(X) dependencies was regarded as indicative of some pre-inversion phase transformations. By analogy, we may interpret extrema of ρ^E_R(T) in Fig. 6 as an evidence of an apparent phase transformation temperature (PTT) inherent to the studied oil/brine mixtures. It should be noted that the specific non-monotonous effects of temperature have not been registered in viscosity studies of oil / water mixtures, reported by other authors [1-3,15], though the fluid's temperatures have been close to those in our measurements (e.g. 5-40^{o}C in Ref. 1). On the other hand, our earlier rheological experiments with unprocessed crude oils [48], toluene solutions of oil vacuum residue

[47], and crude oil / 25% brine mixtures [16] have revealed a universal importance of temperatures ≈28-30^{o}C, supposedly being a signature of some structural phase transitions in an asphaltene/resin subsystem of petroleum-based fluids.

3.6. Volume expansion coefficients of crude oil / brine mixtures

Coefficients of volume expansion $\beta(T) = \frac{1}{V}\frac{dV}{dT}$ for crude oils, brines and mixtures with any water cut were numerically calculated from the original density vs. temperature data sets as $\beta(T_m) = \rho(T_m)\frac{\Delta T}{\Delta \rho}$, where $\Delta\rho = \rho_{i+1} - \rho_i$ and $\Delta T = T_{i+1} - T_i$ are density and temperature increments for consecutive data points, $T_m = (T_{i+1} + T_i)/2$.

Representative β(T) dependencies are shown in Fig. 7a,b,c for the same samples as in Figs. 5,6. These results also indicate the existence of a phase transformation temperature, even in a more straightforward manner, than the $\rho^{E}_{R}(T)$ data of Fig. 6. Namely, in all studied cases, β(T) dependencies for non-mixed oils and brines form two well separated, slowly varying branches. Individual β(T) curves for mixtures with water cuts below 0.3 (not shown in Fig. 7 to avoid a clatter of data points) are also slowly varying and tend to lie close to the respective "Oil" branches, as may be expected, because in natural mixtures with low water cuts crude oil is known to be the continuous phase [4,8,17,21,29]. On the other hand, in all studied mixtures for water cuts with anomalous excess densities, we observed non-monotonic β(T) dependencies with step-like transition between "Oil" and "Brine" branches, as illustrated in Fig. 7 for mixtures with 50% brine content. For samples T6097 (Fig. 7a) and B4899 (Fig. 7c) the transition is from oil-dominated to water-dominated systems above the PTT of about 25-30^{o}C, while for the sample T6199 (Fig. 7b) the transition obviously is in the opposite direction.

3.7. Phase diagrams of crude oil / brine mixtures

To our knowledge, pre-inversion structural transformations have not been reported previously for natural crude oil - brine mixtures, containing only indigenous surfactants, such as asphaltenes. However the existence of specific phase transformations at water cuts close to X≈0.5 (i.e. at water/oil ratios W/O≈1) is well documented for crude oil – brine mixtures containing sufficient quantities of some specially formulated surfactant/cosurfactant additives [19,20,30,31]. Namely, these mixtures may transform into three-phase (Winsor III type) systems with the new (middle) phase being that of a thermodynamically stable, densely packed microemulsion/bicontinuous phase. The details of phase transformations in a particular mixture are strongly dependent on the mixture's temperature, as illustrated in Fig. 8 by a schematic slice of a 3D phase diagram at a fixed surfactant concentration (adapted from Refs. 32,33). The diagram shows the regions of W/O and O/W emulsions, of emulsions in equilibrium with an excess phase (W/O+W, O/W+O), of lamellar (L_α) and bicontinuous (BC) structures. Note, that for water cuts close to 0.5 there exists a "phase inversion temperature" (PIT) of about 45^{o}C.

As indicated in Section 2.2, our density studies have been performed with non-equilibrated samples, prior to a visible onset of any spatial phase separation. Although this technique does not provide proper phase diagrams, information on the phase transformations may be obtained by plotting contours of equal excess densities on temperature – water cut graphs; such contour plots of excess functions are frequently used for describing properties of fluid mixtures (cf. e.g. [34]). Fig. 9 shows some representative contour diagrams for our crude oil – brine samples, plotted on the basis of the measured $\rho^E_R(X)$ and $\rho^E_R(T)$ dependencies (cf. Figs. 5,6). The majority of these

"contour phase diagrams" are topologically similar to various T-X slices of 3D phase diagrams for oil/brine mixtures with added surfactant formulations [32,33].

In particular, for the sample T6097 with large (positive) excess density anomalies (ρ^E_R up to 1.7% , cf. Figs. 5a,6a) contour lines 1 and 2 in Fig. 9a were plotted for ρ^E_R=0.5% and for ρ^E_R=1.2%, respectively. The resulting diagram is fairly symmetrical with respect to a water cut X≈0.45, possesses an apparent "phase transition temperature" PTT≈37^{o}C and closely resembles the phase diagram of Fig. 8. Some further information on the phase behaviour of this sample may be obtained by inspection of the respective volume expansion coefficients (cf. Fig. 7a). In particular, the semi-oval above PTT may be identified with an "oil-dominated" state, while that at lower temperatures – with a "water-dominated" state of the crude oil – brine mixture (cf. Section 3.6).

For those samples which exhibit both positive and negative excess densities, the "contour phase diagrams" are usually much more complex (Fig. 9c,d). However, an inspection of the collection of contour diagrams for all studied samples allows to suggest that this complexity may have some common origin. Namely, a complex contour plot apparently may be regarded as a superposition of two simpler "subdiagrams", each possessing the basic features of the plot shown in Fig. 9a, but somewhat shifted along both (X and T) axes. This observation may be regarded as indicative of an inhomogeneous, bi-modal composition of the respective W/O dispersions. Typical cases of superposition of two "subdiagrams" are contour plots for samples B4899 (Fig. 9c) and B5498 (Fig. 9d). In both cases excess densities are small ($|\rho^E_R|$<0.7%) and predominantly negative, with the exception of the shaded areas; contours 1,2 and 3 are plotted for ρ^E_R=-0.5%, -0.1% and +0.1% respectively. Finally, the contour plot for the sample T6199 (Fig. 9b) evidently belongs to a single (higher

X) "subdiagram". It may be noted that although this sample is also characterised by small excess densities (<0.45%) the values of ρ^E_R remain positive at all studied temperatures (cf. Figs. 5,6).

Summarising, we may conclude, that the experimental studies of pre-inversion phenomena in 12 oilfield brine – crude oil dispersions reveal that some features of these phenomena strongly resemble those conventionally observed in Winsor III-type dispersions due to an emergence of a "middle" microemulsion/bicontinuous phase at W/O ratios close to 1. Surely, such resemblance should not be regarded as an evidence of our W/O dispersions being Winsor-III systems, but the close analogy may indicate a presence of some common physicochemical processes. To substantiate this apparent analogy, we have performed some additional studies of phase separation processes in water/oil dispersions.

3.8. Direct visualisation of a "middle phase" in crude oil / brine mixtures

At the time when the above analysis of the TATNIPINEFT's density/viscosity database was completed, the original 12 samples of Table 1 were no longer available. Hence, phase separation studies were performed with a new crude oil sample from another, geographically close, Tatarstan oilfield – namely from Romashkinskoje reservoir, Aznakajevskaja productive area, well number 24534, sampled at September 2002. Basic properties of this crude are listed at the bottom line of Table 1. Additional data, which may be relevant to interpretation of our observations, are its almost black colour as well as the contents of suspended solids - 0.06 % (555 mg/m^3) and of chloride salts - 0.15% (1388 mg/m^3). Owing to a presence of salts in the crude, we used conventional tap water as a second phase in the studied mixtures.

All studies were performed in standard 10mm cylindrical glass vessels with the mixture's volume of about 10 cm^3, the W/O ratio being close to unity. The two phases were mixed by vigorously shaking and upturning a vessel several times, which resulted in producing a visually homogenous very dark (opaque) liquid. After mixing, the vessels were placed in a vertical position at room temperature (20-22^oC). Unexpectedly, in course of a phase separation no well-defined boundary was observed between the lower free-water phase and the upper (opaque) part of the sample. Instead, transparent water patches appeared independently in various spatially separated regions all over the lower part of the sample. At the first, "swift" stage of water separation the "patchy" volume increased almost linearly with time until, in 4.5 - 5 hours, it amounted to approximately 70 % of the initial volume of the water phase. At longer times separation proceeded much more slowly with a volume increment not exceeding 2% in 48 hours. After removal (by pipette) of the upper homogeneous (as proved microscopically) oil phase it became clear that the process of free water separation occurred via a destruction (coalescence) of a densely packed w/o emulsion with large (3-4 mm) water drops. A characteristic hexagonal-like structure was observed in the upper emulsion layers indicating its high water content of ≥0.74 [35-37]. Water coalescence eventually resulted in an effectively bicontinous composition of the lower part of the sample, partially visible even at the early stages of the "swift" phase separation. Namely, the predominant transparent water phase was almost totally interpenetrated by a delicate 3D foam-like structure with cell walls composed of thin, multiply-punctured films of a dark material, as illustrated in Fig. 10. The characteristic features of the observed complex *macroscopic* emulsion/bicontinuous phase closely resembled the structures, usually revealed by imaging of *microscopic* (submicron) biliqud foams ("gel emulsions") [35,36].

Thin films of “dark subphase” in the foam-like structure could withstand a mechanical stress and demonstrated a high degree of elasticity, as observed by gently shaking and rotating a glass vessel. Samples of these films were collected from broken cells in the bicontinuous regions and microscopic examination revealed that this “subphase” was also a w/o emulsion with a high water content, though with much smaller water droplets. A representative microscopic image of the “dark material” placed on a glass slide is shown in Fig. 11. A characteristic feature of this emulsion is its clearly bimodal character with two well-separated populations of droplets. A quantitative analysis of the image in Fig. 11 shows that larger droplets have a wide distribution centred at ≈40-45 μm, with a “tail” at larger sizes indicating a tendency to coalescence. The most abundant small droplets have a distribution peaked below 7-8 μm (the smaller drops could not be reliably resolved at the photographic image). Fig. 11 also shows that the small water droplets tend to form closely packed structures, usually characteristic to submicron high internal phase ratio emulsions (HIPRE) [35]. Moreover, in Fig. 11 2-D arrays of small droplets encapsulate some larger droplets, evidently providing stabilising action – only slow coalescence effects were observed in this sample even after two weeks-long storage in air. Steric stabilisation of macroscopic water-in-oil droplets by 2D layers of (solid) colloid particles of comparable dimensions is a well known phenomenon in so-called Pickering emulsions [38,39] and images of individual encapsulated droplets with raspberry-like texture (“colloidosomes”) [40,41] resemble some of the structures seen in Fig. 11. We suggest that the “subphase” of the smallest w/o droplets is responsible for formation of the larger-scale densely packed emulsion/bicontinuous phase. Such suggestion is based on the previously reported observations of bimodal emulsions, where dense

arrays of larger drops were formed as a result of a depletion attraction provided by smaller droplets (cf. a review [37] and references therein).

To our knowledge, the formation of the described middle phase, with the structure resembling that of "quasi-biliquid foams" has never been observed in oilfield crude oil – brine mixtures, hence this unusual phenomenon will be a subject of a special detailed investigation. In relation to the present density studies, the preliminary phase separation experiments evidently confirm the above conclusion (cf. Section 3.7) that peaking of excess densities at water cuts of 0.4-0.6 may be the result of formation in crude oil – brine mixtures of dense middle phases with structures resembling those observed in some microemulsions.

3.9. Possible role of asphaltenes in dense "middle phases"

Some evidence of stabilisation of water-in-oil droplets by dense rigid/elastic layers has been presented in earlier publications [7,11,42], while recent studies have shown that this dense phase may possess a highly ordered structure like that in lamellar liquid crystals (cf. a review [12] and references therein). In the above references it is argued that the main constituents of the stabilising dense phase are evidently molecular aggregates of asphaltenes with a possible contribution of fine solids and of naphthenic acids. Kilpatrick and Spiecker [43] postulated that the stabilising phase is a viscous, cross-linked, three-dimensional network of asphaltene aggregates with high mechanical strength. The exact conformation in which asphaltenes organise at oil-water interfaces and the corresponding intermolecular interactions have yet to be agreed upon. The suggested explanations are H-bonding between acidic functional groups, electron donor-acceptor bonding between metal atoms and polar functional groups, π-bonding between delocalised π electrons in

fused aromatic rings. The relative strength and importance of each in forming the interfacial phase in water-in-oil emulsions have still not been fully explained. In the oil phase asphaltenes are peptised by the resinous components. However, when asphaltenic aggregates adsorb to the o/w interface, the resins are evidently shed and do not participate in the stabilising phase [43]. This is in agreement with the observed lack of correlation of the excess densities with the resin content of our crudes (cf. Section 3.3).

In the absence of other solids, the maximum density of a new phase is evidently that of solid asphaltenes ($\rho_A \approx 1.1$ g/cm^3 [44]), while the respective phase volume (and, hence, the maximum value of ρ^E_R) should primarily depend on the asphaltene content of a crude oil. The latter conclusion is supported by the data of Fig. 4 which indicate that for a given water cut the maximum values of ρ^E_R decrease with decreasing asphaltene concentration until below ≈5 wt. % asphaltenes apparently cease to be the determining species at the o/w interface. In oils with low asphaltene contents the properties of the interfacial phase are apparently determined by various non-asphaltene molecules. Differences in sizes and shapes of these molecular species as well as a presence of some weak repulsive interactions may be responsible for the observed negative excess densities [45].

The observed "phase transformation temperatures" (PTT) (cf. Figs.2,6,7,9) also may be attributed (at least partially) to the specific properties of crude oil asphaltenes. Namely, asphaltene colloidal dispersions are known to be sterically stabilised by solvated resins [46]. A structural transformation of asphaltene aggregates may occur when resin molecules "desorb" from asphaltenes. In our previous studies of model crude oils [47,48] we have obtained experimental evidence of a structural phase transition in the asphaltene/resin subsystem at temperatures close to 30 ^{0}C and

suggested two possible effects that trigger the apparent desorption of resins. One is a first-order transition between closely packed and loosely bound structures in the adsorbed layers of resin molecules. Another possible mechanism is the change of the surface energy of π-stacked asphaltene aggregates due to phase transformation of their inner molecular structure. Thermally activated structural transition in asphaltene aggregates, triggered by the destruction of stabilising resin shells at ≈30 ^{0}C also has been regarded as a probable cause of rheological anomalies in bitumen [49].

A particular mechanism of a PTT at ≈30 ^{0}C may be a change of wettability of some solids at the w/o interface. As structurally modified asphaltene particles are no longer fully solvated by resins, they show a higher propensity to adsorb at other solid particles, e.g. at fine solids and at wax crystallites. In particular, when asphaltene aggregates adsorb on the surfaces of wax particles, their wettability changes from completely oil wetting to a mixed (intermediate) wetting; the asphaltene-solvated wax particles migrate to the oil–water interface, contributing to the formation of rigid layers around water droplet and to the emulsion tightness [7,42].

5. Conclusions

The oilfield samples studied were mixtures of 12 degassed (dead) crude oils with respective oilfield brines (formation waters) from Aktanishskoje oil reservoir, Tatarstan, Russia. All unprocessed samples were collected directly from well-heads and contained only indigenous surfactants, such as asphaltenes, resins and fine solids. A conventional viscometer technique did not reveal any structural transformations in pre-inversion brine/water dispersions. On the other hand, by density measurements we observed easily detectable non-zero excess densities and excess thermal expansions for water cuts in the range from X=0.4 to X=0.6 at all studied temperatures of T=5-

50^{o}C. There were definite correlations of the excess values with asphaltene contents and viscosities of crude oils. T-X contour plots of excess densities resulted in diagrams, topologically very close to T-X phase diagrams conventionally observed in some standard Winsor III type systems. We suggest that the observed results are due to a formation of some dense asphaltene-mediated “middle phase” in the studied w/o dispersions. The formation of a complexly-structured foam-like “middle phase” has been directly verified by visual/microscopic studies of a phase separation in a crude oil – water mixture

Acknowledgements

The financial support of the Russian Federation’s Ministry of Education (Grant 206.03.01.051/2003) is greatly appreciated.

References

[1] Viscosity of oil/water mixtures. Project MSDC59, Report No. 263/97. National Engineering Laboratory, East Kilbride, September 1998.

[2] S. Arirachakaran, K.D. Oglesby, M.S. Malinowsky, O. Showam, J.P. Brill, SPE Paper 18836. (1989) 155.

[3] M. Nadler, D. Mewes, Int. J. Multiphase Flow 23 (1997) 55.

[4] L.L. Schramm, (Ed.), Emulsions – Fundamentals and Applications in the Petroleum Industry, American Chemical Society, Washington DC, 1992.

[5] M. Lia, M. Xua, Y. Maa, Z. Wua, A.A. Christy, Fuel 81 (2002) 1847.

[6] Y. Long, T. Dabros, H. Hamza, Fuel 81 (2002) 1945.

[7] M.F. Ali, M.H. Alqam, Fuel 79 (2002) 1309.

[8] Mechanism of the Formation of a Mousse. Petroleum Association of Japan Oil Spill Response Dept. (PAS-OSR). Internet edition: www.pcs.gr.jp / doc / Emousse / text.htm

[9] L.Y. Yeo, O.K. Matar, E.S. Perez de Ortiz, G.F. Hewitt, Multiphase Sci. Technol. 12 (2000) 51 ; Chem. Eng. Sci. 57 (2002) 1069.

[10] J.-L. Salager, in: P. Becher (Ed.), Encyclopedia of Emulsion Technology, Vol. 3, Marcel Dekker, New York, 1988, p.79.

[11] R. Aveyard, B.P. Binks, J.H. Clint, Adv. Coll. Interface Sci. 100-102 (2003) 503.

[12] J. Sjoblom, N. Aske, I.H. Auflem, O. Brandal, T.E. Havre, O. Saether, A. Westvik, E.E. Johnsen, H. Kallevik, Adv. Coll. Interface Sci. 100-102 (2003) 399.

[13] V.A. Muñoz, K.L. Kasperski, O.E. Omotoso, R.J. Mikula, Petrol. Sci. Technol. 21 (2003) 1509.

[14] X. Yang, J. Czarnecki, Abstract 00445, 51st Canadian Chemical Engineering Conference, October 2001.

[15] M. Charles, G.W. Gavier, G.W. Hodgson, Can. J. Chem. Eng. 39 (1961) 27.

[16] I.N. Evdokimov, N.Yu. Eliseev, D.Yu. Eliseev, Fuel 83 (2004) 897.

[17] E. Dahl (coordinator). Handbook of Water Fraction Metering. Revision 1. Oslo: Norwegian Society for Oil and Gas Measurement (NFOGM), 2001.

[18] G. Oddie, H. Shi, L.J. Durlofsky, K. Aziz, B. Pfeffer, J.A. Holmes, Int. J. Multiphase Flow 29 (2003) 527.

[19] L.W. Lake, Enhanced Oil Recovery, Prentice Hall, New Jersey, 1989.

[20] R.C. Nelson, G.A. Pope, SPE Journal 18 (1978) 325.

[21] J. Djuve, X. Yang, I.J. Fjellanger, J. Sjoblom, E. Pelizzetti, Colloid Polym. Sci. 279 (2001) 232.

[22] I. Prigogine, The molecular theory of solution, North Holland, Amsterdam, 1957.

[23] P.J. Flory, J. Am. Chem. Soc. 87 (1965) 1833.

[24] M. Costas, M. Patterson, J. Solution Chem. 11 (1982) 807.

[25] B.P. Tissot, D.H. Welte, Petroleum Formation and Occurrence: A new approach to oil and gas exploration, Springer-Verlag, New York, 1984.

[26] W.B. Russel, D.A. Saville, W.R. Schowalter, Colloidal Dispersions, Cambridge University Press, Cambridge, 1995.

[27] R.C. Ball, P. Richmond, Phys. Chem. Liq. 9 (1980) 99.

[28] G. D'Arrigo, G. Briganti, Phys. Rev. E 58 (1998) 713.

[29] V.F. Medvedev, Collection and preparation of unstable emulsions at oilfields, Nedra, Moscow, 1987. [In Russian]

[30] D.O. Shah, R.S. Schecter (Eds.), Improved Oil Recovery by Surfactant and Polymer Flooding, Academic Press, New York, 1977.

[31] D.H. Smith (Ed.), Surfactant-Based Mobility Control: Progress in Miscible-Flood Enhanced Oil Recovery, American Chemical Society, Washington, 1988.

[32] L. Taisne, B. Cabane, Langmuir 14 (1998) 4744.

[33] W.M. Gelbart, A. Ben-Shaul, J. Phys. Chem. 100 (1996) 13169.

[34] M. Domingues-Perez, S. Freire, J. Jimenes de Llano, E. Rilo, L. Segade, O. Cabesa, E. Jimenez, Fluid Phase Equlibria 212 (2003) 331.

[35] K.J. Lissant, J. Colloid Interface Sci. 22 (1966) 462.

[36] O. Sonneville-Aubrun, V. Bergeron, T. Gulik-Krzywicki, B. Jonsson, H. Wennerstrom, P. Lindner, B. Cabane, Langmuir 16 (2000) 1566.

[37] P.A. Kralchevsky, K.D. Danov, N.D. Denkov, in: K.S. Birdi (Ed.), Handbook of Surface and Colloid Chemistry. 2nd Expanded and Updated Edition, CRC Press, New York, 2002. Ch.5.

[38] J.W. Anseth, A. Bialek, R.M. Hill, G.G. Fuller, Langmuir 19 (2003) 6349.

[39] N.R. Ashby, B.P. Binks, Phys. Chem. Chem. Phys. 2 (2000) 5640.

[40] A.D. Dinsmore, M.F. Hsu, M.G. Nikolaides, M. Marquez, A.R. Bausch, D.A. Weitz, Science 298 (2002)1006.

[41] The University of Warwick. Centre for Interfaces and Materials. Internet Publication: http://www2.warwick.ac.uk/fac/sci/chemistry/cim/research/bon/topics/

[42] M.A. Khadim, M.A. Sarbar, J. Petrol. Sci. Eng. 23 (1999) 213.

[43] P.K. Kilpatrick, P.M. Spiecker, in: Encyclopedic Handbook of Emulsion Technology, J. Sjöblom (Ed.), Marcel Dekker, New York, 2001. p.707.

[44] Y. Bouhadda, D. Bendedouch, E. Sheu, A. Krallafa, Energy Fuels 14 (2000) 845.

[45] R.T. Fort, W.R. Moore, Trans. Farad. Soc. 62 (1966) 1112.

[46] J.G. Speight, J. Petrol. Sci. Eng. 22 (1999) 3.

[47] I.N. Evdokimov, D.Yu. Eliseev, N.Yu. Eliseev, J. Petrol. Sci. Eng. 30 (2001) 199.

[48] I.N. Evdokimov, N.Yu. Eliseev, Chem. Technol. Fuels Oils 35 (1999) 377.

[49] O.G. Uranga, Internet publication, http: //www.rheofuture.de/award/papers.shtm.

Table 1. Properties of crude oil – brine samples used in density studies (12 upper lines) and in phase separation experiments (bottom line).

WELL	DEGASSED CRUDE OIL							BRINE
	Density (20^oC) kg/m^3	Viscosity (20^oC) mm^2/s	MW g/mol	Sulphur wt %	Asphaltenes wt %	Resins wt %	Waxes wt %	Density (20^oC) kg/m^3
T6097	902.2	64.80	250.1	3.68	8.89	19.25	5.59	1153.9
T6098	905.1	69.94	224.3	3.92	3.03	12.65	1.96	1148.2
T6199	904.4	64.34	256.0	4.11	5.13	11.71	3.23	1148.0
B5494	902.4	52.41	250.1	3.30	6.20	11.52	1.42	1174.7
B7695	898.0	49.60	250.1	3.01	7.78	8.60	2.99	1174.7
B0598	897.5	40.93	237.9	3.42	3.85	12.89	2.03	1148.2
B5498	905.4	58.25	246.2	3.29	9.35	10.98	1.86	1148.2
B6698	896.7	42.43	232.5	3.41	3.28	11.45	1.80	1148.2
B4899	904.1	50.72	260.4	4.43	6.04	11.11	12.5	1148.0
B7599	900.5	44.59	277.0	3.32	5.13	11.71	3.23	1152.7
K3396	908.2	66.78	254.1	3.41	4.97	15.60	2.13	1154.9
K4999	906.0	53.10	274.9	3.82	5.35	9.75	12.42	1148.0
Romash	915.0	86.19		2.19	3.29	24.77	2.48	Tap Water

Fig. 1. Filled circles – an experimental viscosity - water cut dependence for sample T6097 at 50^{o}C. Lines – best fits of the Stockes-Einstein linear model (1), of its quadratic expansion (2) and of the Mooney expression for interacting particles (3).

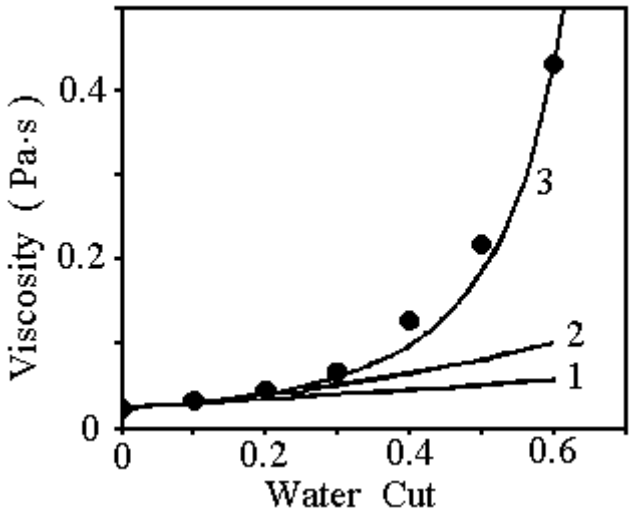

Fig. 2. Temperature dependence of the best-fit Mooney interaction parameters for sample T6097.

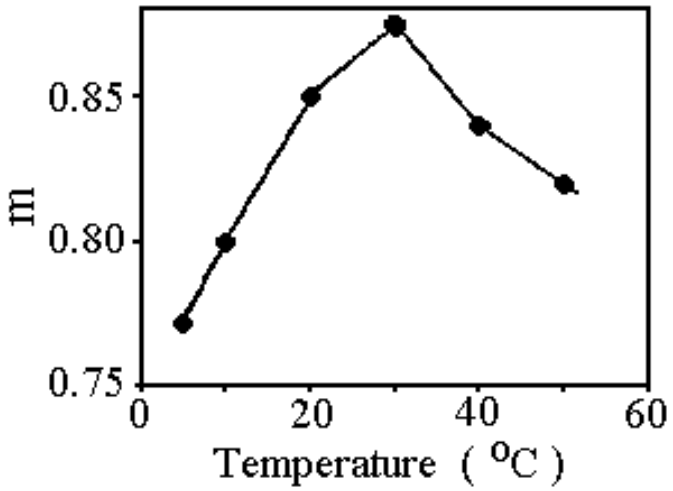

Fig. 3. Water cut effect on the shear-thinning behaviour of viscosity in sample T6097 at 5^{o}C.

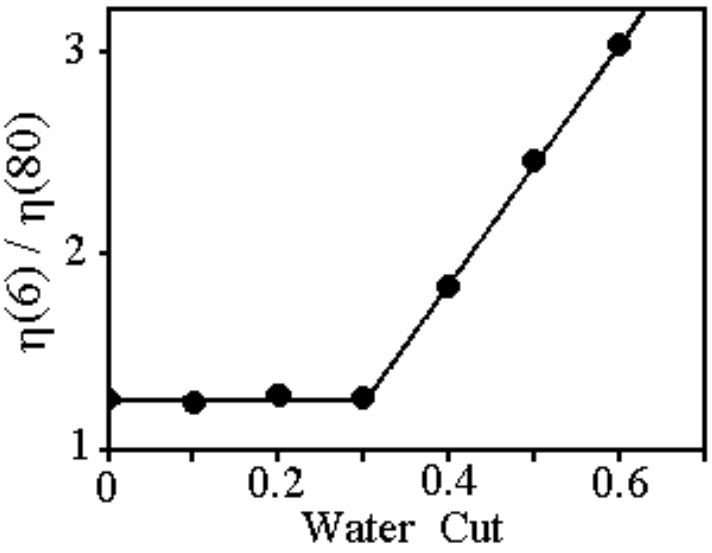

Fig. 4. Correlation of the peak values of relative excess densities in 12 crude oil/brine mixtures with asphaltene contents (wt. %) and kinematic viscosities (mm^2/s) of crude oils.

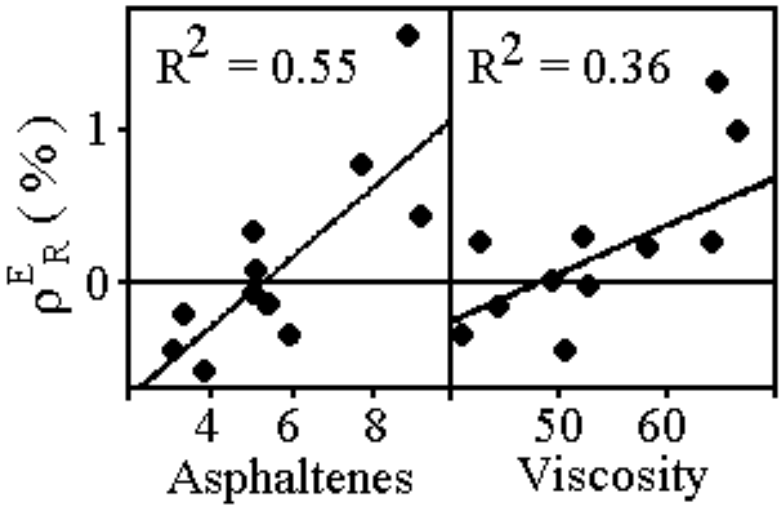

Fig. 5. Water cut effects on the excess densities at 5°C (open circles) and 50°C (filled circles) in samples T6097 (a), T6199 (b) and B4899 (c).

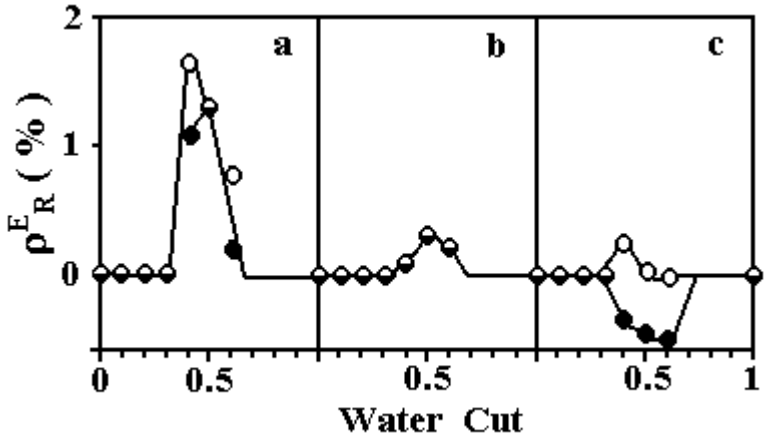

Fig. 6. Temperature effects on the excess densities in samples T6097 (a), T6199 (b) and B4899 (c) at a water cut X=0.4.

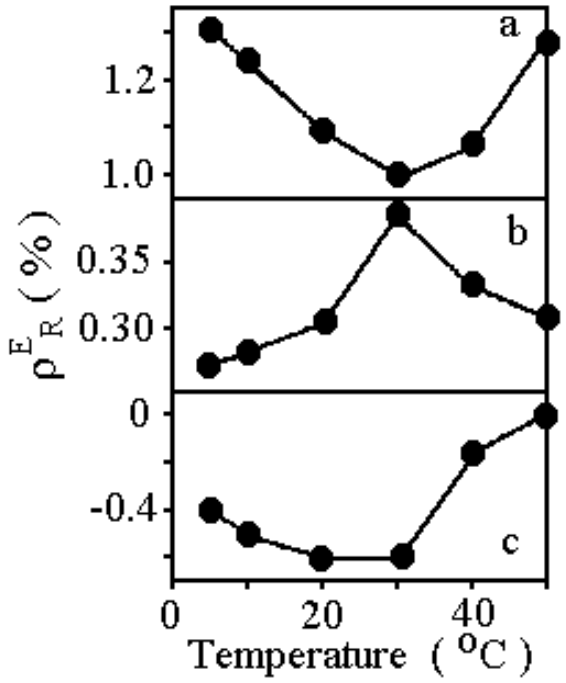

Fig. 7. Temperature effects on volume expansion in samples T6097 (a), T6199 (b) and B4899 (c). Open circles – 100% crude oils and brines; filled circles – 50% oil/brine mixtures.

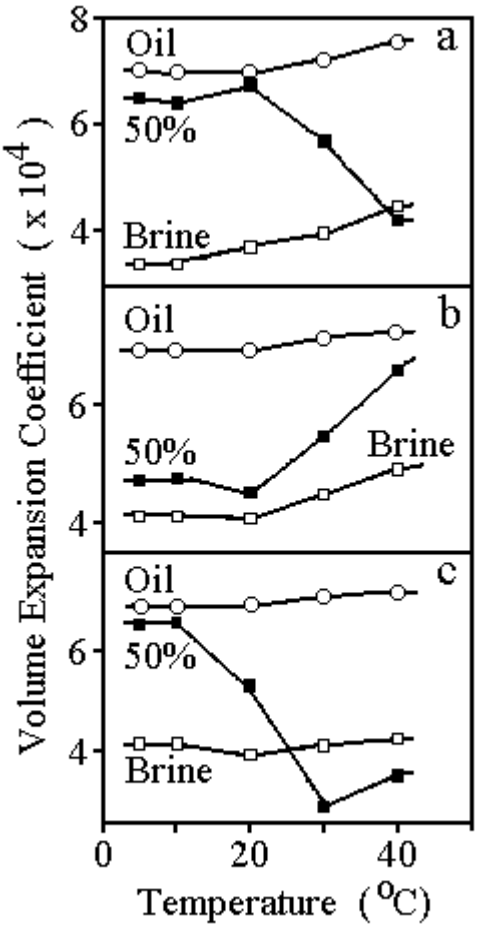

Fig. 8. A typical T-X phase diagram for an oil – water system with specially formulated surfactant/cosurfactant additives (after [32,33]).

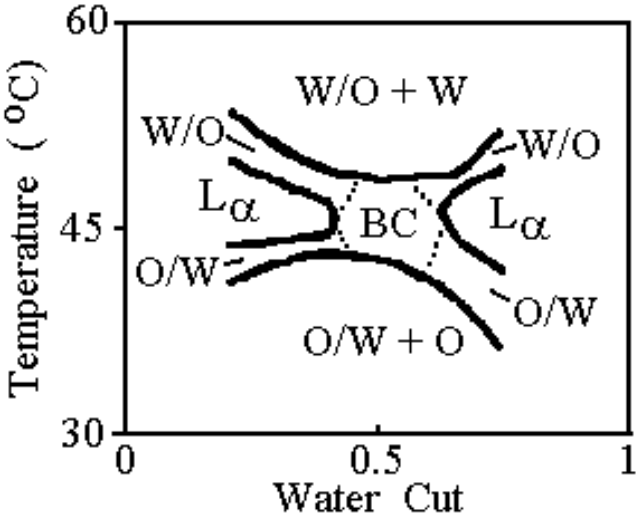

Fig. 9. T-X "contour phase diagrams" (lines of equal excess densities) for samples T6097 (a), T6199 (b), B4899 (c) and B5498 (d).

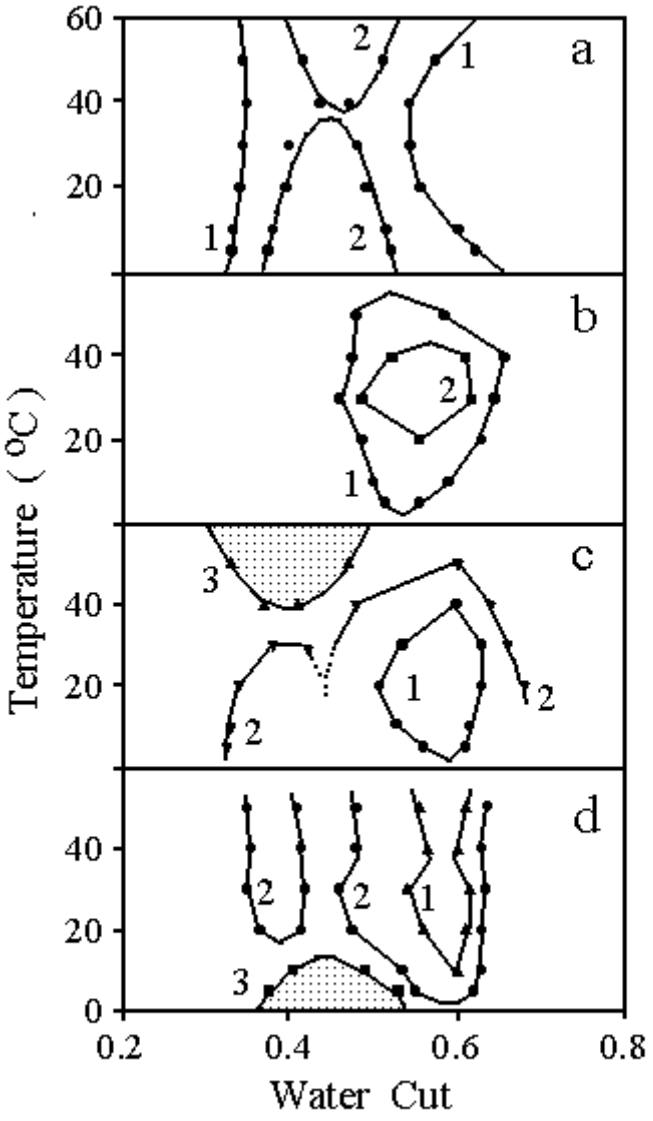

Fig. 10. Transient 3D foam-like structures of thin films between water droplets in a coalescing densely packed w/o emulsion (photos taken through the walls of 12 mm cylindrical glass vessels).

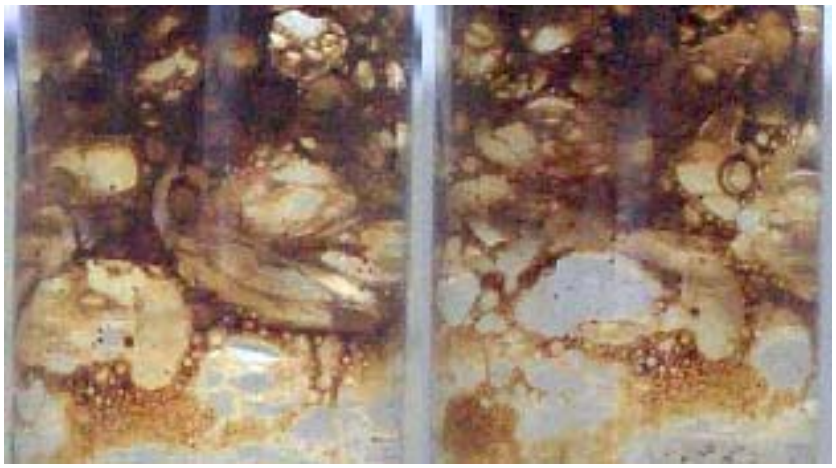

Fig. 11. A microscopic image of the film-forming material in Fig. 10. The horizontal bar denotes 100 micrometers.